

## Low-energy electron collisions with acetic acid

T. C. Freitas,<sup>1,\*</sup> M. T. do N. Varella,<sup>2,†</sup> R. F. da Costa,<sup>2,‡</sup> M. A. P. Lima,<sup>3,4,§</sup> and M. H. F. Bettega<sup>1,||</sup><sup>1</sup>*Departamento de Física, Universidade Federal do Paraná, Caixa Postal 19044, 81531-990 Curitiba, Paraná, Brazil*<sup>2</sup>*Centro de Ciências Naturais e Humanas, Universidade Federal do ABC, Rua Santa Adélia, 166, 09210-170 Santo André, São Paulo, Brazil*<sup>3</sup>*Instituto de Física Gleb Wataghin, Universidade Estadual de Campinas, Caixa Postal 6165, 13083-970 Campinas, São Paulo, Brazil*<sup>4</sup>*Centro de Ciência e Tecnologia do Bioetanol CTBE, Caixa Postal 6170, 13083-970 Campinas, São Paulo, Brazil*

(Received 21 October 2008; published 18 February 2009)

We present cross sections for elastic collisions of low-energy electrons with acetic acid. We employed the Schwinger multichannel method with pseudopotentials in the static-exchange and static-exchange plus polarization approximations, for energies ranging from 0.1 to 10 eV. We found a  $\pi^*$  shape resonance around 1.7 eV, corresponding to the  $A''$  symmetry of the  $C_s$  group. This resonant state was assigned to the experimental dissociative electron attachment peak at 1.7 eV yielding  $\text{CH}_3\text{COO}^- + \text{H}$ . We also performed a series of electronic structure calculations using a small basis set for acetic, formic, and trifluoroacetic acids, which exhibit a similar behavior with respect to the dissociative electron attachment. We believe that hydrogen elimination triggered off by electron capture into a  $\pi^*$  resonance could be a general property of carboxylic acids.

DOI: [10.1103/PhysRevA.79.022706](https://doi.org/10.1103/PhysRevA.79.022706)

PACS number(s): 34.80.Bm, 34.80.Gs

### I. INTRODUCTION

After the discovery by Boudaïffa *et al.* [1,2] that secondary electrons, which are produced by the ionizing radiation, are responsible for single- and double-strand breaks in DNA, studies of electron collisions with biological molecules became an important subject. DNA is a complex system and therefore studies of electron collisions with smaller biological systems (acids, alcohols, hydrocarbons, DNA building blocks) can provide information which help in understanding the behavior of DNA under interactions with slow electrons.

Among the simplest organic molecules we can cite formic ( $\text{HCOOH}$ ) and acetic ( $\text{CH}_3\text{COOH}$ ) acids. Regarding interactions with slow electrons, formic acid has received more attention than acetic acid. Electron collisions with formic acid have been investigated both experimentally [3–6] and theoretically [7–11]. These studies reported a shape resonance around 1.9 eV which is responsible for the dissociative electron attachment (DEA) of formic acid yielding  $\text{HCOO}^-$  and  $\text{H}$  as products. In particular, Rescigno *et al.* [9] elucidated the mechanism for dissociation of the  $\text{O—H}$  bond through the  $\pi^*$  resonance localized on the  $\text{C=O}$  bond. Hydrogen elimination along the  $\text{O—H}$  bond arises from a conical intersection between the  $\pi^*$  ( $A''$ ) anion state and a dissociative ( $A'$ ) anion state, involving symmetric stretch ( $\text{C=O}$ ,  $\text{C—O}$ ) and symmetry breaking (out-of-plane rotation of the  $\text{C—H}$  bond) vibrational modes. The reaction thus takes place in a two-step mechanism, namely, electron capture in the  $\pi^*$  resonance followed by dissociation through a diabatically coupled  $A'$  state.

There are fewer studies concerning electron collisions with acetic acid. Most are experimental studies [3,4,12,13]

and their main focus was in the DEA. Experiments by Pelc *et al.* [3,4], Sailer *et al.* [12], and Prabhudesai *et al.* [13] reported the existence of a shape resonance around 1.5 eV responsible for the DEA yielding  $\text{CH}_3\text{COO}^-$  and  $\text{H}$  as products. Sailer *et al.* [12] reported another low-energy resonance around 0.75 eV that would be responsible for the DEA yielding  $\text{CH}_2\text{O}_2^-$  and  $\text{CH}_2$  as products. In order to help the interpretation of their results, Sailer *et al.* also performed small basis set electronic structure calculations. Based on the results of these calculations they assigned the 0.75 eV resonance to the lowest unoccupied molecular orbital (LUMO) and the 1.5 eV resonance to the  $\text{LUMO}+1$ . The only theoretical study computed ionization cross sections by electron impact of acetic acid using the binary-encounter-Bethe model [14].

Another acid that resembles formic and acetic acids is the trifluoroacetic acid ( $\text{CF}_3\text{COOH}$ ). Langer *et al.* [15] discussed the DEA to trifluoroacetic acid and they found a resonance at around 1 eV which dissociates  $\text{CF}_3\text{COOH}$  into  $\text{CF}_3\text{COO}^-$  and  $\text{H}$ . The DEA for these three acids seems to be similar since processes are triggered off by a  $\pi^*$  resonance located on the  $\text{C=O}$  bond causing a  $\text{O—H}$  bond breaking.

In the present work we report cross sections for low-energy electron collisions with acetic acid from 0.1 to 10 eV. We employed the Schwinger multichannel method with pseudopotentials in the static exchange and in the static exchange plus polarization approximations. Our main purpose is to investigate the existence of shape resonances at low energies and to assign them to the symmetries of the  $C_s$  group. We also carried out electronic structure calculations using a small basis set for acetic, formic, and trifluoroacetic acids. This procedure is often employed in experimental and theoretical works [12,16] and helps in the characterization of shape resonances orbitals and energies. In the present case, these results would help in the discussion on the  $\pi^*$  resonance of acetic acid.

In Sec. II we discuss our computational procedures. We then present and discuss our results, comparing them with

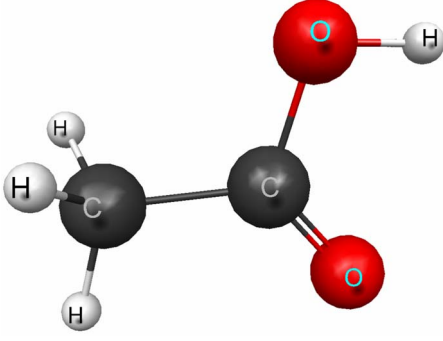
\*tcf03@fisica.ufpr.br

†marcio.varella@ufabc.edu.br

‡romarly.costa@ufabc.edu.br

§maplima@ifi.unicamp.br

||bettega@fisica.ufpr.br

FIG. 1. (Color online) Geometrical structure of  $\text{CH}_3\text{COOH}$ .

available experimental data and with other theoretical results. We end this paper with a brief conclusion.

## II. THEORY

We employed the Schwinger multichannel method (SMC) [17–19] with pseudopotentials [20] to compute the elastic cross sections. Since the SMC method has been described in detail in several publications here we will only discuss the relevant points to the present calculations.

In the SMC method the working expression for the scattering amplitude (in the body frame) is given by

$$f(\vec{k}_f, \vec{k}_i) = -\frac{1}{2\pi} \sum_{m,n} \langle S_{\vec{k}_i} | V | \chi_m \rangle (d^{-1})_{mn} \langle \chi_n | V | S_{\vec{k}_f} \rangle, \quad (1)$$

where the  $\{\chi_m\}$  represents a basis set of  $(N+1)$ -electron symmetry-adapted Slater determinants [configuration-state functions (CSFs)]. These CSFs are constructed from products of target states with one-particle wave functions. For calculations carried out in the static-exchange approximation, the  $(N+1)$ -electron basis set is constructed as follows:

$$|\chi_m\rangle = \mathcal{A}|\Phi_1\rangle \otimes |\varphi_m\rangle,$$

where  $|\Phi_1\rangle$  is the target ground state (represented by a single  $N$ -electron Slater determinant),  $|\varphi_m\rangle$  is an one-electron function, and  $\mathcal{A}$  is the antisymmetrizer. For calculations carried out in the static-exchange plus polarization approximation, the above set is enlarged by CSFs constructed as

$$|\chi_{mn}\rangle = \mathcal{A}|\Phi_m\rangle \otimes |\varphi_n\rangle,$$

where  $|\Phi_m\rangle$  are  $N$ -electron Slater determinants obtained by single excitations from the occupied (hole) orbitals to a set of unoccupied (particle) orbitals.  $|\varphi_n\rangle$  is also an one-electron function and  $\mathcal{A}$  is the antisymmetrizer.

The  $d_{mn}$  matrix elements are given by

$$d_{mn} = \langle \chi_m | A^{(+)} | \chi_n \rangle, \quad (2)$$

and the  $A^{(+)}$  operator can be written as

$$A^{(+)} = \frac{1}{2}(PV + VP) - VG_p^{(+)}V + \frac{\hat{H}}{N+1} - \frac{1}{2}(\hat{H}P + P\hat{H}). \quad (3)$$

In the above equations  $S_{\vec{k}_{i(f)}}$  is an eigenstate of the unperturbed Hamiltonian  $H_0$ , given by the product of a target state

TABLE I. Uncontracted Cartesian Gaussian functions used for carbon and oxygen.

| Type | Carbon exponent | Oxygen exponent |
|------|-----------------|-----------------|
| $s$  | 12.49628        | 16.05878        |
| $s$  | 2.470286        | 5.920242        |
| $s$  | 0.614028        | 1.034907        |
| $s$  | 0.184028        | 0.316843        |
| $s$  | 0.039982        | 0.065203        |
| $p$  | 5.228869        | 10.14127        |
| $p$  | 1.592058        | 2.783023        |
| $p$  | 0.568612        | 0.841010        |
| $p$  | 0.210326        | 0.232940        |
| $p$  | 0.072250        | 0.052211        |
| $d$  | 0.831084        | 1.698024        |
| $d$  | 0.229204        | 0.455259        |
| $d$  | 0.075095        | 0.146894        |

and a plane wave with momentum  $\vec{k}_{i(f)}$ ;  $V$  is the interaction potential between the incident electron and the target;  $\hat{H} \equiv E - H$  is the total energy of the collision minus the full Hamiltonian of the system, with  $H = H_0 + V$ ;  $P$  is a projection operator onto the open-channel space and  $G_p^{(+)}$  is the free-particle Green's function projected on the  $P$  space.

Our calculations were carried out in the static-exchange (SE) and in the static-exchange plus polarization (SEP) approximations. The ground-state molecular geometry was optimized using the package GAMESS [21] at the second-order Møller-Plesset level (MP2) using a TZV++g(2d,p) basis set in the  $C_s$  point group. The geometrical structure of acetic acid is shown in Fig. 1, generated by McMolPlt [22]. We employed the *norm-conserving* pseudopotentials of Bachelet *et al.* [23] to replace the core electrons of carbon and oxygen. The Cartesian Gaussian functions used to represent the target ground state and the scattering orbitals for carbon and oxygen are shown in Table I and were generated according to Ref. [24]. The basis set for hydrogen shown in Table II consists of the 4s (contracted to 3s) basis set of Dunning [25], augmented with one  $p$ -type function with exponent 0.75.

As discussed above, to take polarization effects into account we considered single excitations from the hole (occupied) orbitals to a set of particle (unoccupied) orbitals. In the present calculations we considered all valence occupied orbitals as hole orbitals. We employed modified virtual orbitals

TABLE II. Cartesian Gaussian functions for H.

| Type | Exponent | Coefficient |
|------|----------|-------------|
| $s$  | 13.3615  | 0.130844    |
|      | 2.0133   | 0.921539    |
|      | 0.4538   | 1.0         |
|      | 0.1233   | 1.0         |
| $p$  | 0.7500   | 1.0         |

(MVOs) [26] to represent particle and scattering orbitals, as proposed by Winstead *et al.* [27]. To generate the MVOs we diagonalized a +4 cationic Fock operator. The MVOs were then orthogonalized to the occupied orbitals. To select the MVOs we used as a cutoff criterion the energies of the MVOs. In the present calculations we considered excitations to MVOs with energies less than  $-6$  hartree. The same set of MVOs were used as scattering orbitals. We considered singlet and triplet coupled excitations and obtained 10147 (doublets) CSFs for  $A'$  symmetry and 9217 (doublets) CSFs for the  $A''$  symmetry.

Acetic acid has a permanent dipole moment. The computed value of 1.99 D agrees well with the experimental value of 1.70 D [28]. To take the long-range character of the dipole interaction into account, our differential cross sections were calculated with the Born closure scheme described in Ref. [29]. The lower partial waves of the scattering amplitude (up to  $\ell_{\text{SMC}}$ ) are described with the SMC approach and the higher ones ( $\ell > \ell_{\text{SMC}}$ ) with the Born approximation for the dipole-moment potential. In the present SE calculations, we used  $\ell_{\text{SMC}}=4$  at 3 eV and  $\ell_{\text{SMC}}=5$  at 5, 7, and 10 eV. In the SEP calculations,  $\ell_{\text{SMC}}=3$  at 3 eV and  $\ell_{\text{SMC}}=4$  at 5 eV, and  $\ell_{\text{SMC}}=5$  at 7 and 10 eV. The  $\ell_{\text{SMC}}$  values were chosen to minimize the difference between the differential cross sections (DCS) obtained with and without the Born correction at large scattering angles ( $\theta > 40^\circ$ ).

To analyze the origin of some structures found in the cross section of the  $A'$  symmetry, we employed a procedure developed by Chaudhuri *et al.* [30], consisting of two steps. The first step is the diagonalization of the operator,

$$\tilde{V} \equiv \frac{1}{2}(PV + VP) + \frac{\bar{H}}{N+1} - \frac{1}{2}(\bar{H}P + P\bar{H}), \quad (4)$$

represented in the basis of the configurations  $\{|\chi_m\rangle\}$ , where  $V$  and  $P$  have been defined and  $\bar{H}$  is the same as  $\hat{H}$ , though calculated at a fixed energy, according to Ref. [30]. Once the eigenvalue problem is solved,  $\tilde{V}|\tilde{\chi}_m\rangle = v_m|\tilde{\chi}_m\rangle$ , the eigenvectors associated with the smallest  $|v_m|$  are removed, and the scattering amplitude is obtained with the reduced  $(N+1)$ -particle trial basis,  $\{|\tilde{\chi}_m\rangle\}$ . This procedure has successfully identified and removed spurious structures arising from numerical linear dependence in scattering basis set.

### III. RESULTS AND DISCUSSION

In Fig. 2 we show the integral cross section for the acetic acid obtained in the SE and SEP approximations. These cross sections display three structures. In order to assign these structures to the corresponding symmetries of the  $C_s$  group, we obtained the symmetry decomposition of the cross sections, shown in Fig. 3. There are two structures belonging to the  $A'$  symmetry and one structure belonging to the  $A''$  symmetry.

In order to investigate the origin of the two structures in the  $A'$  cross section, we performed the numerical analysis described above for the SE cross section; a similar analysis for the SEP cross section would be very time consuming. By diagonalizing the operator in Eq. (4) and gradually removing

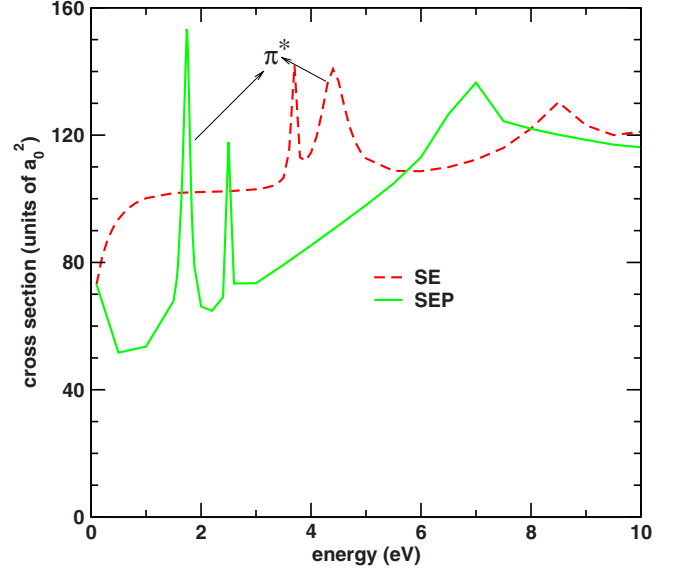


FIG. 2. (Color online) Integral cross section for  $\text{CH}_3\text{COOH}$  in the static-exchange and static-exchange plus polarization approximations. The  $\pi^*$  resonance is indicated by arrows in both cross sections. The other structures are spurious. See text for discussion.

the weakly coupled eigenstates, the structure located around 8.5 eV disappeared. The other structure remained at the same position, though with smaller magnitude. We also found that these two structures are associated with large angular-momentum components;  $\ell=5$  for the structure at lower energy and  $\ell=4$  for the structure at higher energy. In view of these unexpectedly high partial waves and the cross-section

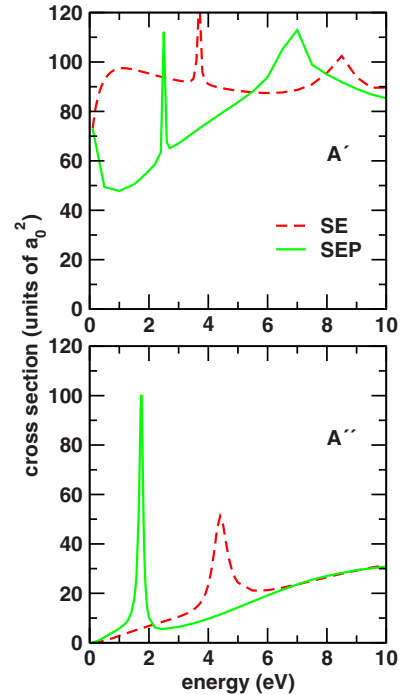


FIG. 3. (Color online) Symmetry decomposition of the integral cross section for  $\text{CH}_3\text{COOH}$  in the static-exchange and static-exchange plus polarization approximations. The two structures belonging to the  $A'$  symmetry are spurious. See text for discussion.

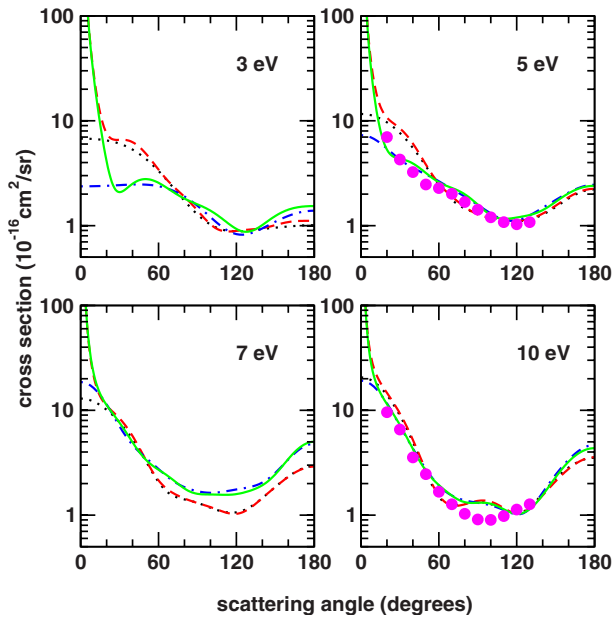


FIG. 4. (Color online) Differential cross sections for acetic acid at 3, 5, 7, and 10 eV. Dotted line (black), SE results without the Born closure; dashed line (red), SE results with the Born closure; dot-dashed line (blue), SEP results without the Born closure; solid line (green), SEP results with the Born closure; circles (magenta), experimental data from Ref. [5] for HCOOH.

behavior upon the removal of singular configurations, we believe these  $A'$  structures are spurious.

In Fig. 4 we show the computed differential cross sections at 3, 5, 7, and 10 eV in the SE and SEP approximations. For both approximations, results obtained with and without the Born correction are shown for comparison purposes. Polarization effects are important at 3, 5, and 7 eV, though SE and SEP results become closer at 10 eV. The long-ranged dipole interaction impacts the differential cross sections at scattering angles below  $\sim 40^\circ$ , as expected. Experimental data of Vizcaino *et al.* [5] for formic acid are also shown in Fig. 4 for comparison, since acetic and formic acid have similar structures,  $R\text{---COOH}$ , with  $R=\text{CH}_3$  and  $R=\text{H}$ , respectively. In general, the calculated cross sections for acetic acid are close to the experimental results for formic acid, suggesting that low-energy electron scattering is dominated by the carboxyl moiety. However, the acetic acid DCS at 10 eV is  $d$ -wave shaped, while formic acid displays a  $p$ -wave pattern; this coupling of higher partial waves could be understood as a fingerprint of the methyl group.

Turning attention to the  $\pi^*$  resonance in the  $A''$  integral cross section (Fig. 3), we note that it shifts from 4.5 eV in the SE approximation to 1.5 eV in the SEP approximation. The

TABLE III. Calculated values for LUMO and LUMO+1 (in hartrees) for acetic, formic, and trifluoroacetic acids.

|                 | $\text{CH}_3\text{COOH}$ | $\text{HCOOH}$ | $\text{CF}_3\text{COOH}$ |
|-----------------|--------------------------|----------------|--------------------------|
| LUMO ( $a''$ )  | 0.1524                   | 0.1335         | 0.0801                   |
| LUMO+1 ( $a'$ ) | 0.2083                   | 0.2030         | 0.1686                   |

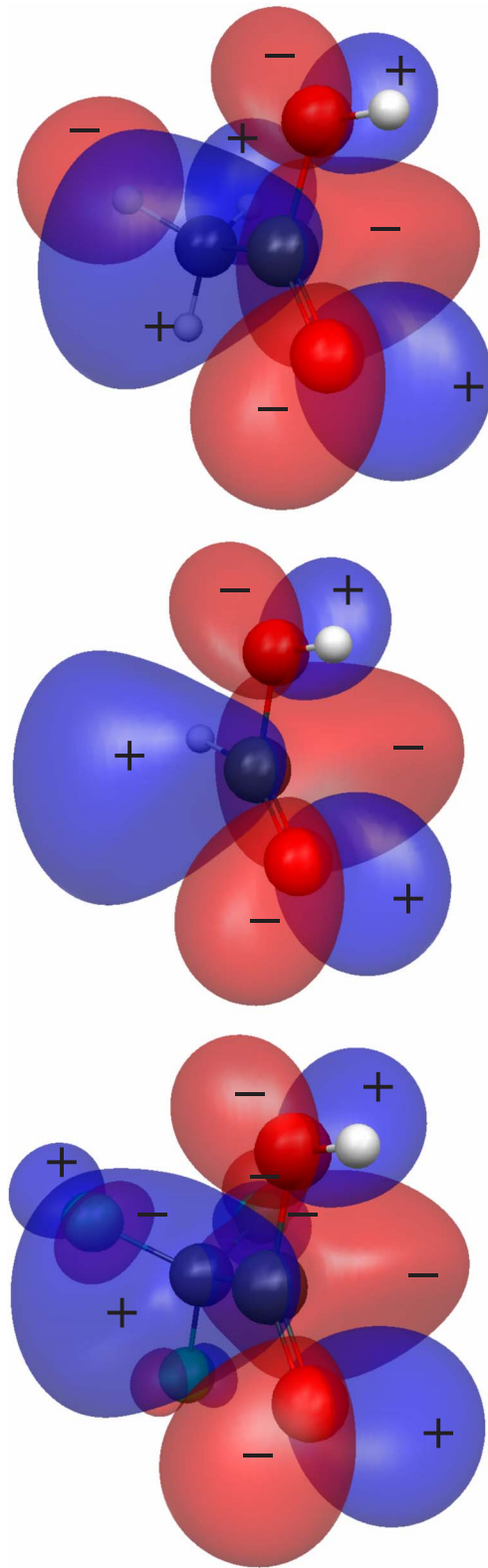


FIG. 5. (Color online) Plots for the LUMO for the three acids. From top to bottom: acetic, formic, and trifluoroacetic acids.

SEP result agrees well with the experimental value of 1.5 eV. Sailer *et al.* [12] reported another resonance around 0.75 eV and claimed it would be responsible for the formation of  $\text{CH}_2\text{O}_2^-$ . With the help of electronic structure calculations,



these authors assigned the resonant features at 0.75 and 1.5 eV to the LUMO and LUMO+1, respectively. We mention that Prabhudesai *et al.* [13] did not observe a resonance around 0.75 eV, and the present calculations do not support the existence of a  $A'$  resonance either.

In order to clarify this point, we carried out electronic structure calculations using GAMESS. Following Sailer *et al.* [12], we optimized the ground-state geometry at the MP2 level of correlation using a 6-31g(1d) basis set and then calculated the energy at the Hartree-Fock level using a double zeta valence basis set. The resulting LUMO and LUMO+1 belong to the  $A''$  and  $A'$  symmetries, respectively. According to these results, the LUMO would be responsible for the formation of  $\text{CH}_3\text{COO}^-$  (the 1.5 resonance), and not of  $\text{CH}_2\text{O}_2^-$  as pointed out by Sailer *et al.* [12]. The  $A''$  LUMO is consistent with a  $\pi^*$  resonance, and though the products of the hydrogen elimination reaction ( $\text{H}_3\text{CCOO}^- + \text{H}$ ) have  $A'$  symmetry, this result can be understood on the basis of the mechanism proposed for dissociation in formic acid, namely, the capture in a  $\pi^*$  resonance diabatically coupled to a dissociative  $A'$  state. Finally, we mention that no resonance at the  $A'$  symmetry was reported by Rescigno *et al.* [9] for formic acid, though a question was raised on the existence of a virtual state.

We also carried out electronic structure calculations for formic and trifluoroacetic acids. Geometry optimizations and Hartree-Fock energies were obtained with the same procedure described above for acetic acid. For both molecules, the symmetry assignments for LUMO and LUMO+1 are the same as in acetic acid ( $A''$  and  $A'$ , respectively). Since trifluoroacetic acid also dissociates into  $\text{CF}_3\text{COO}^- + \text{H}$  products [15], hydrogen elimination triggered off by electron attachment to a  $\pi^*$  orbital could be a general DEA mechanism in carboxylic acids. The energies of LUMO and LUMO+1 for acetic, formic, and trifluoroacetic acids are given in Table III, and the respective LUMO plots (obtained with McMolPit

[22]) are shown in Fig. 5. For the three molecules, the  $A''$  LUMOs have nodal planes, as expected, having similar shapes on the carboxyl moiety ( $\text{C}=\text{O}$  and  $\text{O}-\text{H}$  bonds).

#### IV. CONCLUSIONS

We computed elastic cross sections for low-energy electron collisions with acetic acid. Our results indicate the existence of a  $\pi^*$  resonance ( $A''$  symmetry) around 1.7 eV, related to the experimental DEA peak yielding  $\text{CH}_3\text{COOH}^- + \text{H}$  through the hydrogen elimination mechanism previously proposed for formic acid (capture into a  $\pi^*$  resonance diabatically coupled to a dissociative  $A'$  anion state). The present calculations do not support the existence of a  $A'$  resonance, though. Electronic structure calculations for acetic, formic, and trifluoroacetic acids suggest that the DEA mechanism triggered off by  $\pi^*$  resonances could be a general property of carboxylic acids.

#### ACKNOWLEDGMENTS

T.C.F. acknowledges support from Brazilian agency Coordenação de Aperfeiçoamento de Pessoal de Nível Superior (CAPES). R.F.d.C. would like to acknowledge the financial support from the Brazilian agency Fundação de Amparo à Pesquisa do Estado de São Paulo (FAPESP). M.A.P.L. and M.H.F.B. acknowledge support from Brazilian agency Conselho Nacional de Desenvolvimento Científico e Tecnológico (CNPq). M.H.F.B. also acknowledges support from the Paraná state agency Fundação Araucária and from FINEP (under Project No. CT-Infra 1). T.C.F. and M.H.F.B. acknowledge computational support from Professor Carlos M. de Carvalho at DF-UFPR. The authors also acknowledge support from CENAPAD-SP. Discussions with Dr. Alexandra P. P. Natalense are gratefully acknowledged.

- 
- [1] B. Boudaïffa, P. Cloutier, D. Hunting, M. A. Huels, and L. Sanche, *Science* **287**, 1658 (2000).
  - [2] L. Sanche, *Eur. Phys. J. D* **35**, 367 (2005).
  - [3] A. Pelc, W. Sailer, P. Scheier, N. J. Mason, E. Illenberger, and T. D. Märk, *Vacuum* **70**, 429 (2003).
  - [4] A. Pelc, W. Sailer, P. Scheier, and T. D. Märk, *Vacuum* **78**, 631 (2005).
  - [5] V. Vizcaino, M. Jelisavcic, J. P. Sullivan, and S. J. Buckman, *New J. Phys.* **8**, 85 (2006).
  - [6] M. Allan, *J. Phys. B* **39**, 2939 (2006).
  - [7] F. A. Gianturco and R. R. Lucchese, *New J. Phys.* **6**, 66 (2004).
  - [8] F. A. Gianturco and R. R. Lucchese, *Eur. Phys. J. D* **39**, 399 (2006).
  - [9] T. N. Rescigno, C. S. Trevisan, and A. E. Orel, *Phys. Rev. Lett.* **96**, 213201 (2006).
  - [10] C. S. Trevisan, A. E. Orel, and T. N. Rescigno, *Phys. Rev. A* **74**, 042716 (2006).
  - [11] M. H. F. Bettega, *Phys. Rev. A* **74**, 054701 (2006).
  - [12] W. Sailer, A. Pelc, M. Probst, J. Limtrakul, P. Scheier, E. Illenberger, and T. D. Märk, *Chem. Phys. Lett.* **378**, 250 (2003).
  - [13] V. S. Prabhudesai, D. Nandi, A. H. Kelkar, and E. Krishnakumar, *J. Chem. Phys.* **128**, 154309 (2008).
  - [14] P. Mozejko, *Eur. Phys. J. Spec. Top.* **144**, 233 (2007).
  - [15] J. Langer, M. Stano, S. Gohlke, V. Foltin, S. Matejcek, and E. Illenberger, *Chem. Phys. Lett.* **419**, 228 (2006).
  - [16] See, for example, M. Allan and L. Andric, *J. Chem. Phys.* **105**, 3559 (1996); P. D. Burrow, G. A. Gallup, and A. Modelli, *J. Phys. Chem. A* **112**, 4106 (2008); C. Winstead and V. McKoy, *Int. J. Mass Spectrom.* **277**, 279 (2008).
  - [17] K. Takatsuka and V. McKoy, *Phys. Rev. A* **24**, 2473 (1981).
  - [18] K. Takatsuka and V. McKoy, *Phys. Rev. A* **30**, 1734 (1984).
  - [19] M. A. P. Lima, L. M. Brescansin, A. J. R. da Silva, C. Winstead, and V. McKoy, *Phys. Rev. A* **41**, 327 (1990).
  - [20] M. H. F. Bettega, L. G. Ferreira, and M. A. P. Lima, *Phys. Rev. A* **47**, 1111 (1993).
  - [21] M. W. Schmidt, K. K. Baldrige, J. A. Boatz, S. T. Elbert, M. S. Gordon, J. H. Jensen, S. Koseki, N. Matsunaga, K. A. Nguyen, S. J. Su, T. L. Windus, M. Dupuis, and J. A. Montgomery, *J. Comput. Chem.* **14**, 1347 (1993).

- [22] B. M. Bode and M. S. Gordon, *J. Mol. Graph. Model.* **16**, 133 (1998).
- [23] G. B. Bachelet, D. R. Hamann, and M. Schlüter, *Phys. Rev. B* **26**, 4199 (1982).
- [24] M. H. F. Bettega, A. P. P. Natalense, M. A. P. Lima, and L. G. Ferreira, *Int. J. Quantum Chem.* **60**, 821 (1996).
- [25] T. H. Dunning, Jr., *J. Chem. Phys.* **53**, 2823 (1970).
- [26] C. W. Bauschlicher, *J. Chem. Phys.* **72**, 880 (1980).
- [27] C. Winstead, V. McKoy, and M. H. F. Bettega, *Phys. Rev. A* **72**, 042721 (2005).
- [28] *CRC Handbook of Chemistry and Physics*, 79th ed., edited by D. R. Lide (CRC, Boca Raton, FL, 1998).
- [29] M. A. Khakoo, J. Blumer, K. Keane, C. Campbell, H. Silva, M. C. A. Lopes, C. Winstead, V. McKoy, R. F. da Costa, L. G. Ferreira, M. A. P. Lima, and M. H. F. Bettega, *Phys. Rev. A* **77**, 042705 (2008).
- [30] P. Chaudhuri, Marcio T. do N. Varella, C. R. C. de Carvalho, and M. A. P. Lima, *Phys. Rev. A* **69**, 042703 (2004).